



## TENSILE PROPERTIES OF COLD METAL TRANSFERRED ARC WELDED AA6061-T6 ALUMINIUM ALLOY JOINTS

\*Addanki Ramaswamy<sup>1</sup>, Malarvizhi S<sup>2</sup> and Balasubramanian V<sup>3</sup>

<sup>1</sup>Research scholar, <sup>2</sup>Associate Professor, <sup>3</sup>Professor, Centre for Materials Joining and Research, Department of Manufacturing Engineering, Annamalai University, Annamalai Nagar - 608 002.

### ABSTRACT

The wide usage of 6xxx series aluminium alloys in automobile sector is mainly because of the exceptionally good weldability characteristics and better corrosion resistance. Cold metal transfer (CMT) arc welding process is an advanced variant of gas metal arc welding (GMAW) that has potential features such as low heat input and arc stability with an innovative wire feed system. This process is widely employed in automobile sector due to its higher welding speed and capability to weld thin sheets without defects like spatter, distortion and burn through. This article reports the welding of thin aluminium sheets (AA6061-T6) by cold metal transfer arc welding technique and presents the transverse tensile properties of the welded joints. The features of the microstructure are characterized by optical microscopy. The fracture surfaces are being examined by scanning electron microscopy. Microhardness survey was done along the cross section of the welded joint. During the tensile test, the welded joint failed at 12 mm from the center of the weld. It is clear that fracture is caused by softening in HAZ region by the formation of  $\beta'$  or  $\beta$  precipitates which are softer and incoherent in nature. The hardness results signify that the low hardness region was found in the HAZ region which is called as softened zone, where the transformation of precipitates or coarsening of grains takes place.

**Keywords:** Aluminium alloy, Gas metal arc welding, Cold metal transfer, Tensile properties, Microhardness

### 1. Introduction

AA6061 is a prominent heat treatable alloy among the 6xxx series aluminium alloys that is widely used in the fabrication of automobile sheet panels, due to the better formability and weldability characteristics [1]. Due to the wide usage of thin aluminium sheets in the fabrication of hood and door components in automobile sector, welding of these thin sheets without any defects is essential. In general welding of thin aluminium sheets is commonly done by the gas metal arc welding process (GMAW) in short circuiting mode to avoid the distortion and burn through issues. However the spatter generation is the serious issue for the producers in manufacturing a component. Therefore a low heat input process like cold metal transfer (CMT) arc welding which encounters the spatter problem by the retraction of wire movement during the short circuiting phase is considered. CMT welding process is a type of GMAW variant which operates mainly in the short circuiting mode by the forward and backward movement of the wire.

Whenever the short circuit happens, the digital processing control disturbs the power supply and therefore the wire can be retracted. This wire retraction mechanism helps the droplet to detach from the wire in short circuiting phase without any electromagnetic force [2]. Therefore the heat input can be controlled in short circuiting phase. Due to the low heat input, the problems like spatter, distortion and wider HAZ can be controlled.

C. G. Pickinet al [3] proved that CMT-GMAW exhibits low thermal input and high wire melting coefficient when compared with the pulsed GMAW process. Pang [4] et al stated that the CMT process is a stable and spatter-free droplet transfer process by control of current parameters. A. Elrefaey [5] suggested that the mechanical properties of the joints welded with CMT-GMAW process are comparatively higher than that of GTAW and GMAW processes. Feng-yuan SHU et al [6] reported that the CMT-GMAW process is mainly suitable to weld thin aluminum alloy sheets due to the

\*Corresponding Author - E- mail: ramaswamy\_311@yahoo.com

low energy (heat input) process and the slight deformation.

Ahmed Elrefaey et al [7] pointed out that the joint made with cold metal transfer welding process gives better joint efficiency with good tensile strength and ductility. They further stated that the microstructure of the HAZ region in CMT-GMA welded joint was almost similar to the base material due to the low heat input. Beytullah Gungor et al [8] claimed that CMT-GMA welded joints produces better joint efficiency with higher welding speed. Jicai Feng et al [9] stated that spatter less weld joint with less deformation and good gap bridge ability is produced with CMT-GMA welding of thin sheets. Zhanget al [10] observed that during the arcing phase in CMT-GMA cycle, the droplet is detached from the wire by means of electromagnetic force caused by retraction of wire movement which stabilizes the weld. Javier Serranoetal [11] investigated the GMAW of AA6061-T6 aluminium alloys and claimed that microstructural transformation of harder precipitates like  $\beta''$  to soft precipitates like  $\beta'$  is the main probable reason for the existence of soft zone in the HAZ region.

Moreover they stated that the formation of voids has been controlled by adopting the electromagnetic stirring force in the weld pool. This electromagnetic stirring action enhances the tensile properties of the welded joints. The hardness decrease in the HAZ region is due to the thermodynamic instability of fine  $\beta''$  needle shaped precipitates to rod shaped  $\beta'$  precipitates. R.R.Ambrizet al [12] reported that higher dilution rates are achieved by adopting the electromagnetic stirring process for the formation of  $Mg_2Si$  precipitates. They also concluded that finer grain size in the weld metal is attributed to the fast cooling rate.

Even though lot of works have been done by various researchers on CMT arc welding of aluminium alloys, but no article highlights the tensile properties of CMT welded joints. Therefore this article provides the indepth study of the tensile properties of the CMT welded AA6061-T6 aluminium alloy joints.

## 2. Experimental Work

AA6061-T6 aluminium alloy as a base material of 3 mm thickness and AA4043 as a filler metal of 1.2 mm diameter were chosen in this investigation. These aluminium sheets were sectioned using a hack saw to make the sheets to the required dimensions of 150 mm length and 75 mm width with a total groove angle of  $60^\circ$ . Chemical composition and mechanical properties of

base material are presented in table 1 and 2 respectively.

Pure argon (99 wt%) was used as a shielding gas. CMT advanced 4000R was used to fabricate the joints. The parameters used to weld the specimens are presented in table 3.

The photograph of the welded joint is as shown in figure 1. The scheme of extraction of specimens from the welded joint is as shown in figure 2. Notch and smooth tensile specimens were prepared as per the ASTM E8-04 as shown in the figure 3. 100 kN electro-mechanical controlled universal testing machine was used to perform the transverse tensile testing at a strain rate of  $1.3 \times 10^{-3} \text{ s}^{-1}$ . Microhardness survey was done using a Vickers microhardness tester with an indentation load of 100 grams at a dwell time of 15 seconds. To reveal the microstructure of the welded specimen, the sample was initially ground with 400 and 800 grit SiC papers and then polished with 6  $\mu\text{m}$  diamond paste to make it mirror polish. Finally the specimen was etched with a solution of 75 HCl, 25  $\text{HNO}_3$ , 5 HF and 25  $\text{H}_2\text{O}$  (ml). Microstructural features of the welded joint were characterized by optical microscopy and fracture surfaces were examined by SEM fractography. Image J software was used to measure the grain size in the weld metal (WM), heat affected zone (HAZ) and partially melted zone (PMZ) regions.

## 3. Results

### 3.1 Tensile Properties

The photograph of the tensile tested specimen showing the fracture location is shown in figure 4. The transverse tensile properties were evaluated by taking the average of three specimens and the results are presented in table 4. Engineering stress strain graph for both the base material and CMT-GMA welded joint is as shown in figure 5. The base material records yield strength (YS) of 275 MPa and an ultimate tensile strength (UTS) of 318 MPa with an elongation of 16 %. The photograph of the tensile tested specimen is as shown in figure 4. From the failed specimen it is clearly visible that the specimen is failed in HAZ region which gives a clear approach that low hardness will be expected. The failure is occurred at 12 mm from the center of the weld. It is clear that fracture is caused by softening in HAZ region by the formation of  $\beta'$  or  $\beta$  precipitates. The CMT-GMA welded joint exhibits a tensile strength of 215 MPa with an elongation of 9.02 %.

**Table 1 Chemical composition (wt %) of the base metal and filler metal**

Material	Si	Cu	Fe	Mn	Mg	Cr	Zn	Ti	Al
AA6061-T6	0.56	0.31	0.28	0.052	0.98	-	0.024	0.018	Bal.
ER4043	5.6	0.3	0.8	0.05	0.05	0.05	0.1	0.02	Bal.

**Table 2 Mechanical properties of the base metal and filler metal**

	0.2% Yield strength (MPa)	Ultimate Tensile strength (MPa)	Elongation in 50 mm gauge length (%)	Hardness (HV <sub>0.1</sub> )
AA6061-T6	275	318	16	120
ER4043	164	190	-	-

**Table 3 Optimized welding parameters used to fabricate the joints**

Process	Welding current (A)	Arc voltage (V)	Arc length correction (%)	Wire feed speed (mm/min)	Welding speed (mm/min)	Heat input (kJ/mm)
CMT-GMAW	116	14	15	5600	480	0.177



**Fig.1 Photograph of the CMT-GMA welded joint.**

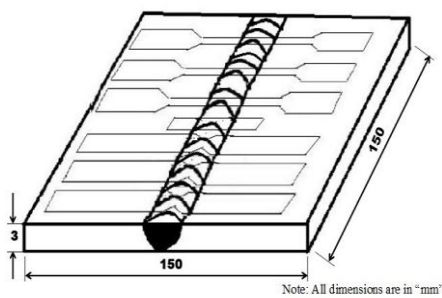


**Fig. 2 Scheme of extraction of the tensile specimens.**

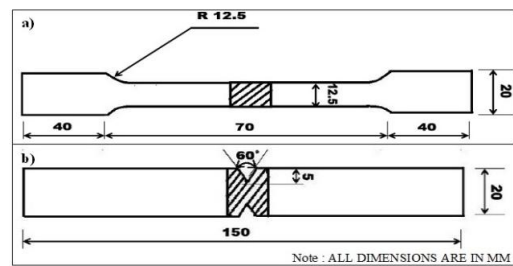


**Fig.3 Dimensions of the tensile specimens  
a) Smooth tensile specimen b) notch tensile specimen**

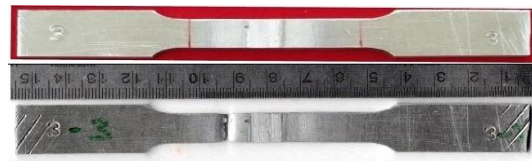


**Fig.4 Photograph of the tensile specimens before and after test.**

This shows that 32.3 % reduction in tensile strength and 43.6 % reduction in elongation compared with the base material. The reduction in cross-sectional area (c.s.a) for the base material is 26.6 %. But the reduction in cross sectional area for the CMT-GMA welded joint is 58 %.

The base material shows a notch tensile strength (NTS) of 325 MPa. But the joint made with CMT-GMA welding process records a NTS of 220 MPa. It shows that 32.3 % reduction in NTS compared with the base material. The notch strength ratio (NSR) is 1.02 for the base material. It is almost same for the CMT-GMA welded joint. This signifies that the joints are insensitive to notches and considered to be fall into notch ductile category since the NSR is greater than one. A joint efficiency of 67.8 % is recorded for CMT-GMA welded joint. This implies that the CMT-GMA welded joint is 32.2 % lower than the base material.

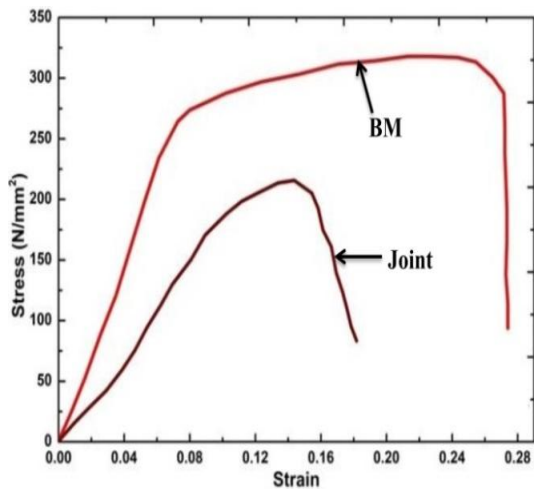


Fig.5 Engineering stress-strain graph for base metal and joint

### 3.2 Microhardness

The microhardness test was performed along the cross section of the joint to determine the variation of microhardness values with a load of 0.01 kg at a gap of 0.5 mm between each indentation. The microhardness distribution profile is shown in the figure 6. The parent material exhibits a hardness value of 120 HV. The hardness value is very low in the HAZ region which signifies that these results are in good agreement with the failure location. A hardness value of 70 HV is recorded in the HAZ region in which the low hardness region was observed with a value of 60 HV. This

confirms that a softened zone is formed in the HAZ region where the hardness is 50 % less than the base material. A hardness of 75 HV is recorded in the weld metal which is slightly larger than the HAZ region.

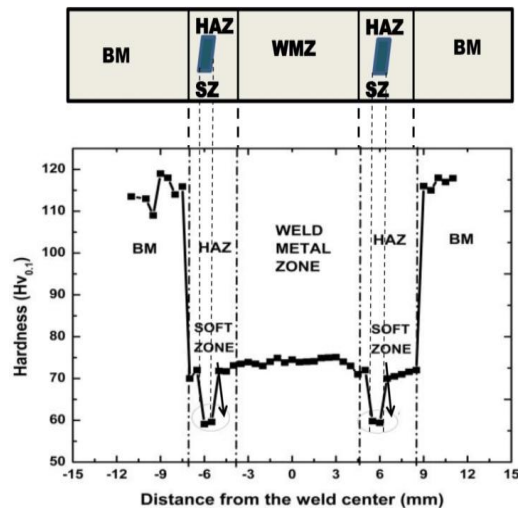


Fig.6 Microhardness distribution of the CMT welded joint

### 3.3 Macro and Microstructure

The macrostructure of the welded joint with various zone microstructures is as shown in figure 7. The macrostructure shows weld bead with aesthetic appearance of deeper penetration and narrow width. No macro level defects were observed. It was also observed that reinforcement height is more for this joint. This is due to the high deposition rate of the CMT-GMA welding process.

The weld joint consists of various zones like WM zone, HAZ, PMZ. The microstructure of the base material consists of equiaxed and elongated grain structure along the rolling direction. HAZ region consists of coarser equiaxed grain structure whereas PMZ is characterized by equiaxed to columnar grain structure at the interface and columnar grain structure at the WM region was observed. Columnar grains which grew towards the center of the weld existed on the interface of the weld metal. Rao et al [13] pointed out that the PMZ area was heated above the solidus temperature and eutectic remelted during welding. Grain size of various zones of the CMT-GMA welded joint is tabulated in table 5. The grain size in HAZ was larger than that in PMZ because HAZ region was exposed to temperature for long intervals of time.

**Table 4 Transverse tensile properties of the weld joint**

Process	0.2% Yield strength (MPa)	Ultimate Tensile strength (MPa)	Elongation in 50 mm gauge length (%)	Reduction in c.s.a. %	Notch tensile strength (MPa)	Notch strength ratio	Joint efficiency (%)	Fracture location
BM	275	318	16	26.6	325	1.02	-	-
CMT-GMAW	175	215	9.02	58	220	1.02	67.6	HAZ

**Table 5. Grain size ( $\mu\text{m}$ ) of various zones of the CMT-GMA welded joint**

Variant	Average grain size ( $\mu\text{m}$ ) in WM	Average grain size ( $\mu\text{m}$ ) in HAZ	Average grain size ( $\mu\text{m}$ ) in PMZ
CMT-GMAW	20.3	47.4	41.7

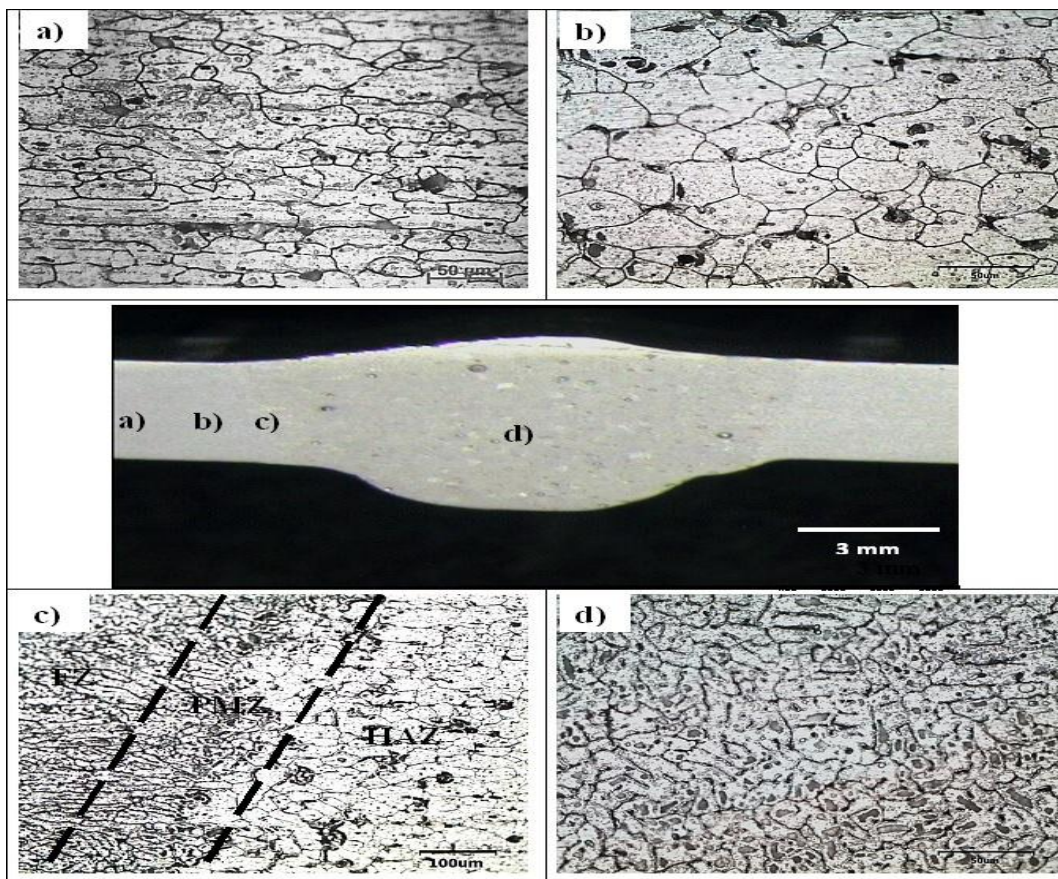


**Fig.7 Optical micrographs of the various regions of the CMT welded joint**

Parent metal    b) HAZ    c) WM-HAZ interface    d)WM

### 3.4 Fracture Surface Analysis

To determine the mode of failure, SEM analysis was done on the fracture surfaces of the tensile tested specimens. The SEM fractographs of the smooth and notch tensile specimens are as shown in figures 8 and 9 respectively. Tearing fibres and ridges in bulk volume fraction are seen on the fracture surface of the base material. This indicates that intense plastic flow occurs in the base material before it fails. The fracture surfaces of the smooth tensile specimens are characterized by deep dimples with very less volume percentage of tear ridges which suggest that the mode of failure is ductile. Whereas the fracture surfaces of the notch tensile specimens consists of long and flat regions of elongated grains separated by tear ridges in ductile manner.

### 4. Discussions

The reduction in tensile strength of the CMT-GMAW joint compared with the base material is due to the heat input that causes vaporization of magnesium from the weld metal even though silicon is present as pointed out by Lakshminarayanan et al. [14] This vaporization of magnesium is due to the higher solid solubility of magnesium compared with the silicon in aluminium alloys. The decrease in ductility of the CMT-GMAW joint compared with the base material is observed. This behaviour is due to the formation of porosity caused by the entrapment of hydrogen gas in the weld pool during the solidification process. In fusion welding process, the process of solidification of the weld pool plays a significant role. It starts from the PMZ with the equiaxed growth of grains towards the fusion boundary.

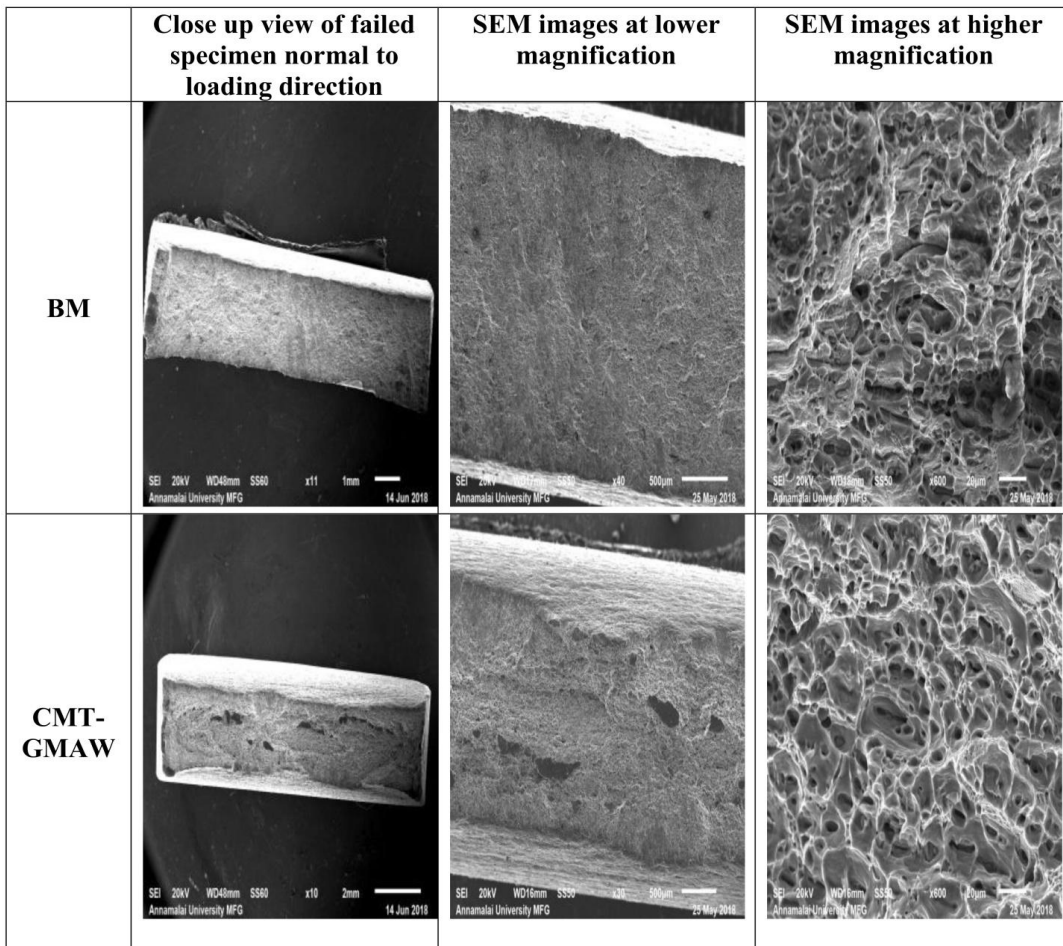


Fig.8 SEM fractographs of the smooth tensile specimens.

The PMZ region acts as a site for the growth of grains rather than the nucleation of grains. Therefore the growth rate is more than the nucleation rate in the PMZ region. This epitaxial growth of grains along the weld pool results in long and oriented columnar grains. Equiaxed to columnar grain structure is formed in the PMZ region. Epitaxial growth requires minimal degree of under cooling prevails. The CMT-GMAW joint is characterized by high cooling rates, which influence several aspects of weld metal solidification. In general the presence of fine columnar grain structure in the weld metal zone of CMT-GMAW joint is due to the high cooling rates associated with the low heat input. While

the coarser equiaxed grain structure is observed in the HAZ region because of the thermal cycling effect. The grain sizes of various zones are presented in the table 5 which says that the grain sizes are in the order of  $FZ < BM < PMZ < HAZ$ . From the Hall-Petch equation, it is well known that the smaller the grain size, the better the mechanical properties, since the Hall-Petch equation is a relation between strength and the grain size. The variation of hardness across the cross section of the weld joint is due to the dissolution or growth of hardening precipitates.

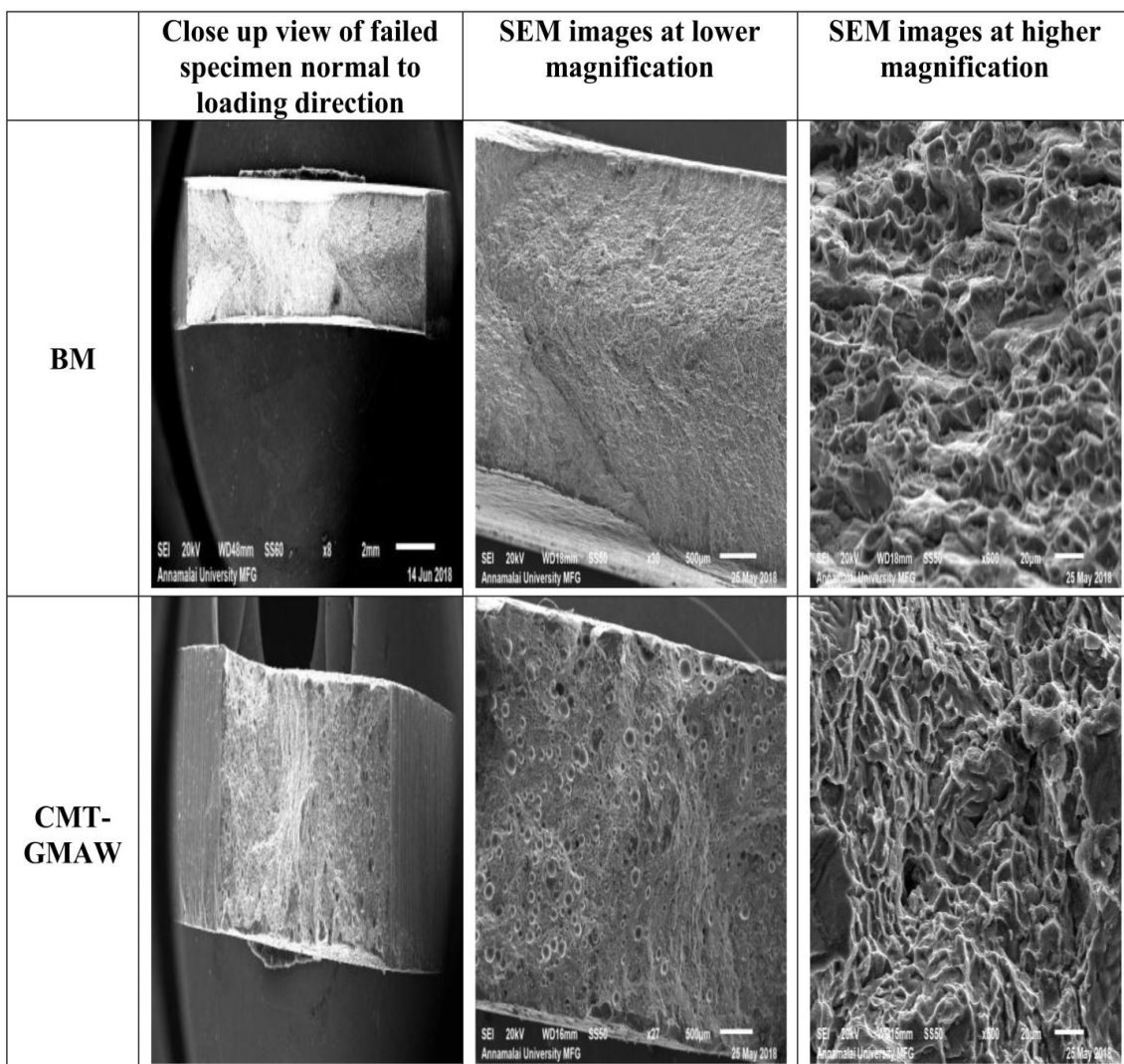


Fig 9. SEM fractographs of the notched tensile specimens

The higher hardness is recorded in the WM region compared with the HAZ region even though the hardening precipitates like  $\beta''$  ( $Mg_5Si_6$ ) are completely dissolved in this region. This is due to the enrichment of the solid solution with Mg and Si in this region. Whereas the lowest hardness is recorded in the HAZ region since most of the solid solution strengthening elements like Mg, Si, Cu are vaporized or segregation of magnesium along the grain boundary. It is also observed that fracture of the joint takes place at a particular point in the HAZ region. This point is named as the softened zone where the complete transformation of  $\beta''$  ( $Mg_5Si_6$ ) to  $\beta$  ( $Mg_2Si$ ) takes place or partial dissolution of precipitates or coarsening of the grains. Similar observation was confirmed by Malin [15]. It is well known that the incoherent precipitates like  $\beta$  in aluminium alloy results in the decrease in the mechanical properties, since the dislocations need an extra stress to pass through the coherent precipitates like  $\beta''$ . However the dislocations bend and finally the matrix deforms relatively ease due to the loss of coherency precipitates. This can be well explained by Porter and Easterling [16].

## 5. Conclusions

1. Transverse tensile properties of CMT welded joint are lower than the base material and the failure occurred in the HAZ region due to the dissolution or transformation of hardened precipitates.
2. A softened zone is formed in the HAZ region where the lowest hardness is recorded due to the complete transformation of hardened precipitates to softened precipitate. The location of the failure matching with this zone.
3. The fracture surfaces of tensile specimens made from CMT welded joint consists of deep dimples which suggests that the failure happened in the ductile mode with considerable amount of plastic deformation before the failure.

## Acknowledgement

The authors wish to thank the Science and Engineering Research Board (SERB), DST, Government of India for providing the financial support through an R&D project No.: SB/S3/MMER/0108/2013 to carry out this investigation.

## References

1. Polmear I, St John D, Nie J F and Qian M (2017), *Light alloys: "Metallurgy of Light metals" 5th edition, BOOK, Butterworth-Heinemann Publications.*
2. Lei H Y, Li Y B and Carlson B E (2017), "Cold metal transfer spot welding of 1 mm thick AA6061-T6", *J. Manuf. Process*, Vol. 28, 209–219.
3. Pickin C G and Young K (2006), "Evaluation of cold metal transfer (CMT) process for welding aluminium alloy", *Sci. Technol. Weld. Join*, Vol. 11, 583–585.
4. Wang P, Hu S, Shen J and Liang Y (2017), "Characterization the contribution and limitation of the characteristic processing parameters in cold metal transfer deposition of an Al alloy", *J. Mater. Process. Technol.*, Vol. 245, 122–133. doi:10.1016/j.jmatprotec.2017.02.019.
5. Elrefaey A (2015), "Effectiveness of cold metal transfer process for welding 7075 aluminium alloys", *Sci. Technol. Weld. Join*. Vol. 20, 280–285. doi:10.1179/1362171815Y.0000000017.
6. Shu F Y, Lü Y H, Liu Y X, Xu F J, Sun Z, He P and Xu B S (2014), "FEM modeling of softened base metal in narrow-gap joint by CMT+P MIX welding procedure", *Trans. Nonferrous Met. Soc. China*, Vol. 24, 1830–1835. doi:10.1016/S1003-6326(14)63260-X.
7. Elrefaey A and Ross N G (2015), "Microstructure and mechanical properties of cold metal transfer welding similar and dissimilar aluminum alloys", *Acta Metall. Sin.* Vol. 28, 715–724.
8. Gungor B, Kaluc E, Taban E, SIK A Ş Ş (2014), "Mechanical and microstructural properties of robotic Cold Metal Transfer (CMT) welded 5083-H111 and 6082-T651 aluminum alloys", *Mater. Des.* Vol. 54, 207–211.
9. Feng J, Zhang H and He P (2009), "The CMT short-circuiting metal transfer process and its use in thin aluminium sheets welding", *Mater. Des.* Vol. 30, 1850–1852.
10. Zhang C, Li G, Gao M, Yan J, Zeng X Y (2013), "Microstructure and process characterization of laser-cold metal transfer hybrid welding of AA6061 aluminium alloy", *Int. J. Adv. Manuf. Technol.* Vol. 68, 1253–1260.
11. Pérez J S, Ambriz R R, López F F C, Viguera D J (2016), "Recovery of Mechanical Properties of a 6061-T6 Aluminum Weld by Heat Treatment After Welding", *Metall. Mater. Trans. A Phys. Metall. Mater. Sci.* Vol. 47, 3412–3422.
12. Ambriz R R, Barrera G, García R and López V H (2009), "A comparative study of the mechanical properties of 6061-T6 GMA welds obtained by the indirect electric arc (IEA) and the modified indirect electric arc (MIEA)", *Mater. Des.* Vol. 30, 2446–2453.
13. Prasad Rao K, Ramanaiah N and Viswanathan N (2008), "Partially melted zone cracking in AA6061 welds", *Mater. Des.* Vol. 29, 179–186.
14. Lakshminarayanan A K, Balasubramanian V and Elangovan K (2009), "Effect of welding processes on tensile properties of AA6061 aluminium alloy joints", *Int. J. Adv. Manuf. Technol.* Vol. 40, 286–296.
15. Malin V (1995), "Study of Metallurgical Phenomena in the HAZ of 6061-T6 Aluminum Welded Joints", *Weld. J*, Vol 74(9). 305–318.
16. Porter D A, Easterling K E and Sherif Y (2009), "Phase Transformations in Metals and Alloys". BOOK, CRC Press.